Influence of forced convection on solidification and remelting in the developing mushy zone

Influence of forced convection on solidification and remelting in the developing mushy zone

M Wu[1,2,a], A Vakhrushev[1], A Ludwig[2] and A Kharicha[1,2]
[1]Christian-Doppler Lab for Adv. Process Simulation of Solidification & Melting,
University of Leoben, Franz-Josef-Str. 18, A-8700 Leoben, Austria
[2]Chair of Simulation and Modeling of Metallurgical Processes,
University of Leoben, Franz-Josef-Str. 18, A-8700 Leoben, Austria

Email: [a]menghuai.wu@unileoben.ac.at

Abstract. The mushy zone and solid shell formed during solidification of a continuous casting are mostly uneven, and this unevenness of shell growth might lead to surface defects or breakout. One known example is the unevenness of shell growth at the impingement point between the jet flow (coming from submerged entry nozzle) and the solidification front. This phenomenon is primarily understood as the local remelting caused by the superheat of the melt, which is continuously brought by the jet flow towards the solidification front. A recent study of the authors [Metall. Mater. Trans. B, 2014, in press] hinted that, in addition to the aforementioned superheat-induced local remelting (1), two other factors also affect the shell growth. They are (2) the advection of latent heat in the semi-solid mushy zone and (3) the enhanced dissipation rate of energy by turbulence in the bulk-mush transition region. This paper is going to perform a detailed numerical analysis to gain an insight into the flow-solidification interaction phenomena. Contributions of each of the above factors to the shell formation are compared.

1. Introduction

The industry practice of continuous casting shows that the mushy zone and solid shell formed during solidification are mostly uneven, and this unevenness of shell growth might lead to surface defects or breakout in the worst case. Reasons for this are diverse: (1) the non-uniform heat flux from the casting to the mould [1-2]; (2) fragmentation of dendrites in the partially solidified shell [3-4]; (3) the dynamic flow-solidification interaction which leads to suppression of solidification or remelting locally [5-7]. The topic of non-uniform heat flux has drawn the significant attention of researchers [8-10]. For the fragmentation of dendrites due to forced convection, some preliminary knowledge [11-13] is also available. The current paper is going to perform numerical studies to gain an insight into the flow-solidification interaction which leads to suppression of solidification or remelting.

   One known example of the unevenness of shell growth during continuous casting is the flow-solidification interaction at the impingement point between the jet flow (coming from the submerged entry nozzle) and the solidification front. According to B.G. Thomas [5-6], this can be primarily explained by the local remelting due to the superheat of the melt, which is continuously brought by the jet flow. A recent study of the authors [7] hinted that, in addition to the aforementioned superheat-induced local remelting; two other factors also affect the shell growth. They are: the advection of latent heat by the melt flow which is co-related to the motion/deformation of the

semi-solid mushy zone and the enhanced dissipation rate of energy by turbulence in the bulk-mush transition region.

2. Key features of the numerical model and benchmark settings

An enthalpy based model [14-18] was used and extended by the current authors for thin slab casting [7]. Deformation of the partially solidified strand shell which affects the interdendritic melt flow is taken into account. We do not repeat all conservation equations, only the enthalpy equation

$$\frac{\partial}{\partial t}(\rho h) + \nabla \cdot (\rho \vec{u} h) = \nabla \cdot (\lambda_{\text{eff}} \nabla T) + S_{\text{e}} , \tag{1}$$

where

$$S_{\text{e}} = \rho L \frac{\partial f_{\text{s}}}{\partial t} + \rho L \cdot \nabla (\vec{u}_{\text{s}} f_{\text{s}}) .$$

This equation is used to calculate the sensible enthalpy of the liquid-solid mixture $h_{\text{mixture}}^{\text{sensible}}$ (written as h hereafter), which represents the volume average of the sensible enthalpies of both liquid and solid phases: $h = f_{\ell} h_{\ell}^{\text{sensible}} + f_{\text{s}} h_{\text{s}}^{\text{sensible}}$. A further model simplification is made by assuming that the liquid and solid have the same sensible enthalpy ($h_{\ell}^{\text{sensible}} = h_{\text{s}}^{\text{sensible}} = h$). During solidification the latent heat (L) is treated separately by considering two source terms, as described in equation (1). In this study we set both liquid and solid the same density (ρ). Thermal conductivity (λ) is also calculated by phase volume averaging, and for the turbulent flow an effective thermal conductivity λ_{eff} ($= \lambda + \lambda_{\text{t}}$) is used to account for the turbulence enhanced energy dissipation.

A critical point of equation (1) is that it includes three different velocities: the intrinsic liquid velocity $\vec{u}_{\ell}$, solid velocity $\vec{u}_{\text{s}}$ and mixture velocity $\vec{u}$. They are related by

$$\vec{u} = f_{\ell} \vec{u}_{\ell} + f_{\text{s}} \vec{u}_{\text{s}} . \tag{2}$$

The mixture velocity is the solution of the momentum equation. The solid velocity is calculated with an incompressible rigid viscoplastic model on the basis of an assumed moving boundary condition [6]. From equation (2) we can derive the intrinsic liquid velocity ($\vec{u}_{\ell}$). Mass and volume conservations apply, i.e. $\nabla \cdot \vec{u} = 0$ and $f_{\ell} + f_{\text{s}} = 1$. The evolution of the solid phase (f_{s}) is determined by the temperature according to the $f_{\text{s}} - T$ function (here the lever rule is used).

Focus of the paper is on the flow-solidification interaction. Three factors affecting solidification are investigated: the superheat (casting temperature over liquidus) induced suppression of solidification or remelting, the advection of latent heat by the interdendritic flow ($-\rho L \nabla \cdot (f_{\ell} \vec{u}_{\ell})$, i.e. $\rho L \nabla \cdot (f_{\text{s}} \vec{u}_{\text{s}})$) and the enhanced dissipation rate of energy by turbulence (λ_{t}). A 2D benchmark as defined in the previous publication [7] is used, as shown in figure 1. A constant turbulence, kinetic energy (2.5 x 10^{-4} m^2 s^{-2}) and a constant dissipation rate (9.3 x 10^{-4} m^2 s^{-3}) are applied at the pressure inlet. A binary alloy (Fe-0.34 wt.%C) is considered, and its physical properties are listed in table 1. Four simulations are performed as listed in table 2.
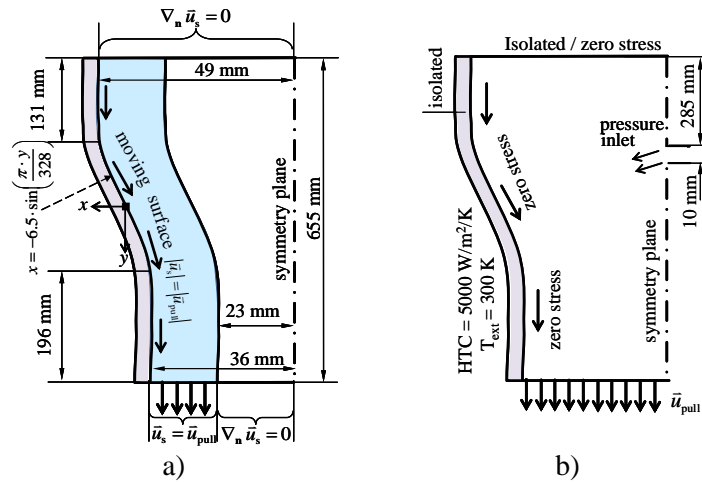
Figure 1. Configuration of a 2D benchmark (a) for calculation of the solid velocity and (b) for the flow-solidification. The geometry in the vertical direction is scaled-down by 1/8. Reproduced from [7].

Table 1. Properties and parameters for the calculations of the 2D benchmark (Fe-0.34 wt.%C).

Thermal physical properties	Thermodynamic data
$c_p = 808.25$ J·kg^{-1}·K^{-1}	$c_0 = 0.34$ wt.% C
$\lambda = 33.94$ W·m^{-1}·K^{-1}	$T_{liquidus} = 1781.8$ K
$\rho = 7027$ kg·m^{-3}	$T_{solidus} = 1710.8$ K
$\mu_\ell = 5.6 \times 10^{-3}$ kg·m^{-1}·s^{-1}	$f_s - T$ function with the level rule.
$L = 2.5 \times 10^5$ J·kg^{-1}	
Process parameters	
$T_{inlet} = 1850$ K	$\vec{u}_{pull} = 0.07$ m·s^{-1}

Table 2. Parameter study of the flow-solidification interaction.

	superheat (K)	source term of latent heat	$f_s^{integral}$ ***
Case I	68.2	S_e	0.0841
Case II	1	S_e	0.1111 (+32%)
Case III*	68.2	disregarding $\rho L \nabla \cdot (f_s \vec{u}_s)$ in S_e	0.1331 (+58%)
Case IV**	68.2	S_e	0.0955 (+14%)

* Identical to case I, but $\rho L \nabla \cdot (f_s \vec{u}_s)$ in S_e is ignored.

** Identical to case I, but in the energy conservation equation the contribution of the turbulence to the effective thermal conductivity (λ_t) is ignored.

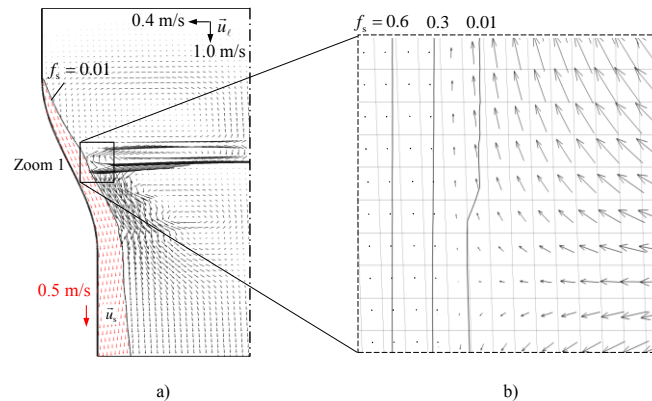*** $f_s^{integral}$: volume average of f_s over the whole calculation domain at steady state.

Figure 2. Result of flow pattern in Case I. a) $\vec{u}_s + \vec{u}_\ell$ (geometry in the vertical direction is scaled-down by 1/8); b) Zoom 1, ($\vec{u}_\ell$ - $\vec{u}_s$) (geometry 1/1 scale). Some isolines of f_s are marked in figure.

3. Results and discussions

Figure 2 shows the calculated velocity fields of case I. The solid velocity is almost parallel to the curved mould surface. A jet flow coming from the inlet impinges on the solidification front, and the solidification front is slightly concaved at the impingement point. Figure 2(b) shows the details of the flow near and in the mushy zone. The flow can penetrate into the mush, but the interdendritic flow is significantly 'dampened' in the vicinity of the solidification front.

3.1 Influence of superheat

Comparison of the steady state solidification profiles between case I and II was made in figure 3: the former with a superheat of 68.2 K, the latter with a superheat of 1 K. It is clear that the higher superheat slows down the solidification. Taking the integral of f_s over the whole calculation domain, we get 32% solid phase with case II more than that with case I (table 2). With the current benchmark configuration, no notable remelting is evidenced.

3.2 Importance of advection of latent heat

Comparison of the steady state solidification profiles between case I and III was made in figure 4: the former with full source term S_e, the latter ignores the part $\rho L \nabla \cdot \left(f_s \vec{u}_s \right)$ from S_e. Overestimation of the shell growth by case III when the advection of latent heat due to the motion of solid phase in the mushy zone is ignored is huge: about 58% (table 2). The latent heat advection term, $\rho L \nabla \cdot \left(f_s \vec{u}_s \right)$, can also be written as $\rho L \vec{u}_s \cdot \nabla f_s$, as $\nabla \cdot \vec{u}_s \equiv 0$. The sign of this term can be '+' or '-', depending on the scalar product of the solid velocity vector $\vec{u}_s$ and the solid fraction gradient ∇f_s.

– A '+' sign indicates that this positive source term in the enthalpy equation will lead to an increase of the sensible enthalpy. The temperature might increase, with a corresponding decrease in the local cooling process. The consequence of this is that the solidification will slow down and even remelting could occur.

– A '-' sign indicates that this negative source term in the enthalpy equation will lead to a decrease of the sensible enthalpy. The temperature might decrease, with a corresponding increase in the local cooling process. The consequence of this is that the solidification will speed up.
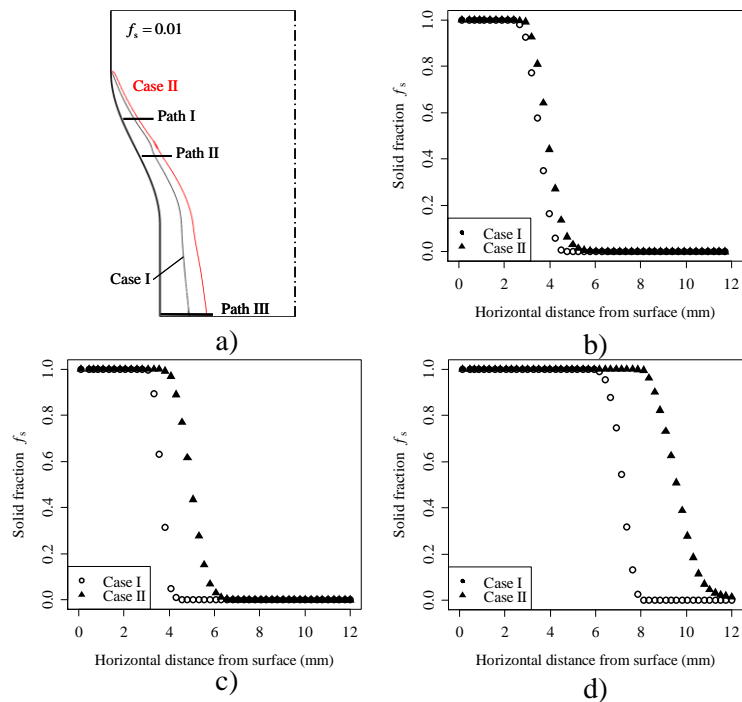
Figure 3. Influence of superheat on the shell growth: comparison of f_s distribution between case I and II. (a) Schematic of solidification front (f_s =0.01); f_s profiles along path I (b), path II (c), path III (d). The paths are 266, 323, 649 mm from top surface, correspondingly.
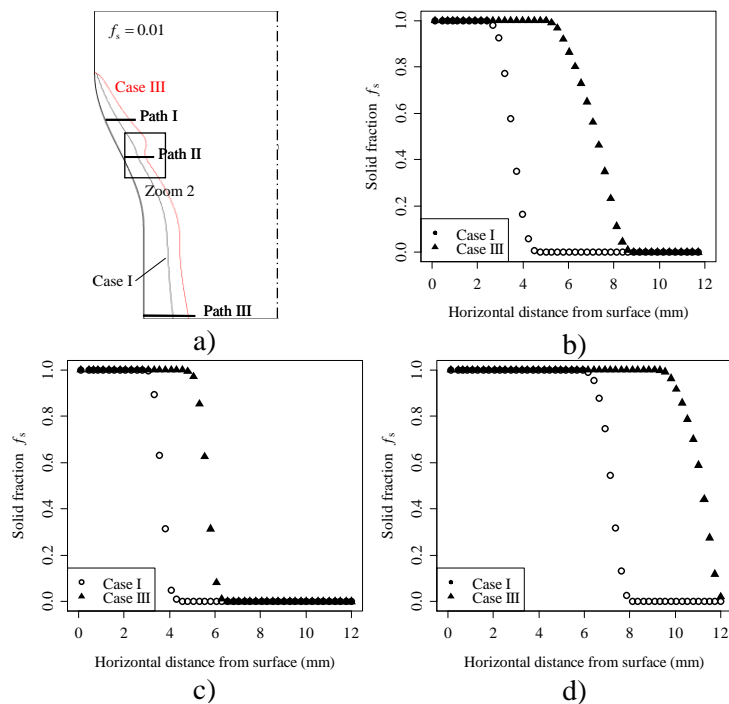

Figure 4. Influence of latent heat advection on the shell growth: comparison of f_s distribution between case I and III. (a) Schematic of solidification front (f_s =0.01); f_s profiles along path I (b), path II (c), path III (d). The paths are 266, 323, 649 mm from top surface, correspondingly.

The calculated $\rho L \vec{u}_s \cdot \nabla f_s$ for case III is shown by the colour scale in figure 5. The term of $\rho L \vec{u}_s \cdot \nabla f_s$ was actually disregarded from the energy equation in this case. It means that in the region with a '+' sign, a depression of solidification or remelting should occur due to this term, but this suppression of solidification or remelting is ignored; therefore it leads to an overestimation of the solidification. In contrast, in the region with a '-' sign, a speed-up of solidification should occur, but this speed-up of solidification is ignored by case III; therefore it leads to an underestimation of the solidification.
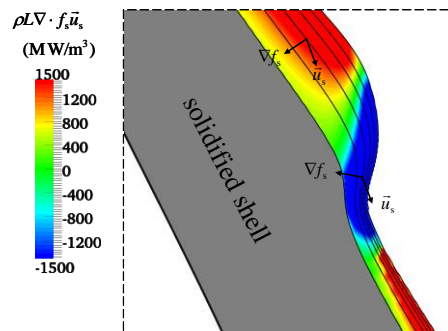

Figure 5. Alignment of the solid volume fraction gradient and the solid velocity vector in the mush zone (case III) in the Zoom 2, as marked in figure 4(a). Isolines of f_s = 0.01, 0.2, 0.4, 0.6, 0.8, 0.99 are shown. The $\rho L \vec{u}_s \cdot \nabla f_s$ term, which is actually ignored in case III, is shown by the colour scale.

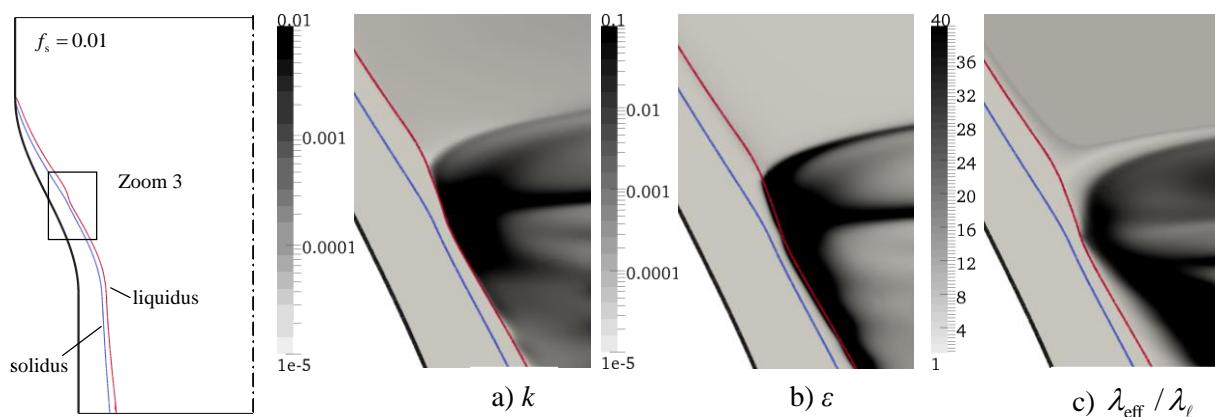a) k b) ε c) $\lambda_{eff} / \lambda_\ell$

Figure 6. Calculated distributions of (a) turbulence kinetic energy, (b) dissipation rate and (c) normalized effective thermal conductivity in zoom 3 of case I.

3.3 Influence of turbulence

Case IV is identical to case I, but in the energy conservation equation of case IV the contribution of the turbulence (λ_t) to the effective thermal conductivity (λ_{eff}) is ignored. Generally, the turbulence-induced energy dissipation suppresses the solidification, which is observed especially in the lower domain below the jet impingement point. If we ignored this turbulence-induced energy dissipation, the solidification could be overestimated by about 14% (table 2). Details of the turbulence quantities for case I are shown in figure 6. The predicted effective thermal conductivity in the bulk melt region and near the jet impingement point can reach as much as 37 times higher than the physical value of the thermal conductivity.

4. Summary discussion

- A numerical parameter study using an enthalpy based solidification model gives an insight into the interaction between the forced convection and solidification in the developing mushy zone. Three influencing factors are analyzed: superheat induced suppression of solidification or remelting, advection of latent heat due to interdendritic flow which is coupled with the motion/deformation of semi-solid mushy zone and turbulence enhanced energy dissipation.

- A 2D benchmark is designed for this study:

- Turbulence suppresses the solidification due to the fact that the turbulence dissipation enhances the diffusive energy transfer. An ignorance of this part of energy transfer would lead to an overestimation of the solidification by 14%.

- Superheat (casting temperature over the liquidus) suppresses the evolution of the mushy zone (growth of the semi-solid shell). For example, a 68.2 K of superheat coming from inlet slows down the solidification by 32% if compared to 1 K of superheat.

- The advection of latent heat in the mushy zone plays a very important role in the formation of the mushy zone (shell). With the motion/deformation of the semi-solid shell, the advection of latent heat in the mushy zone can cause acceleration or depression of the solidification, depending on the interdendritic flow direction and the gradient of the volume fraction solid.

- People have used an "equivalent heat capacity model" [19] for solidification, in which the advection of latent heat due to the interdendritic flow is ignored. This model was successfully applied in many casting processes where the solidified phase is stationary, i.e. ingot castings and shape castings. We learnt that this kind of model cannot be used for continuous casting where the semisolid shell moves.

Acknowledgment

References

[1]   Savage J 1962 *J. Iron Steel Institute* **200** 1962 41-51
[2]   Meng Y and Thomas BG 2003 *Metall. Mater. Trans.* **34B** 685-705
[3]   Lesoult G, Combeau H and Moukassi M 1993 *Journal de Physique IV* **3** 813-822
[4]   Hellawell A, Liu S and Lu SZ 1997 *JOM* **49(3)** 18-20
[5]   Koric A, Thomas BG and Voller VR 2010 *Numer. Heat Transf. B Fundam.,* **57** 396-413
[6]   Zhao B, Thomas BG, Vanka SP and O'Malley RJ 2005 *Metall. Mater. Trans.* **36B** 801-823
[7]   Vakhrushev A, Wu M, Ludwig A, Tang Y, Hackl G and Nitzl G 2014 *Metall. Mater. Trans.* **45B** in press, DOI: 10.1007/s11663-014-0030-2
[8]   Cho J, Shibata H, Emi T and Suzuki M 1998 *ISIJ Int.* **38** 440-446
[9]   Camporredondo-S JE, Castillejos-E AH, Acosta-G FA, Gutierrez-M EP and Herrera-G MA 2004 *Metall. Mater. Trans.* **35B** 443-457
[10] O'Connor TG and Dantzig JA 1994 *Metall. Mater. Trans.* **25B** 541-560
[11] Yamazaki M, Natzume Y, Harada H and Ohsasa K 2006 *ISIJ Int.* **46** 903-908
[12] Campanella T, Charbo C and Rappaz M 2004 *Metall. Mater. Trans.* **35A** 3201-3210
[13] Su Z, Chen J, Nakajima K and He J 2009 *Steel Res Int.* **80** 824-833
[14] Prescott PJ and Incropera FP 1994 *J. Heat Transfer* **116** 735-741
[15] Prescott PJ, Incropera FP and Gaskell DR 1994 *Trans. ASME* **116** 742 – 749
[16] Prescott PJ and Incropera FP 1995 *Trans. ASME* **117** 716 – 724
[17] Voller VR and Prakash C 1987 *Int. J. Heat Mass Transfer* **30** 1709 – 1719
[18] Voller VR, Brent AD and Prakash C 1989 *Int. J. Heat Mass Transfer* **32** 1719 – 1737
[19] Hsiao JS 1985 *Numer. Heat Transf.* **8** 653-666